

$J = 14$  Hz), 1.50 (s, 3 H), 1.39 (s, 6 H), 1.20 (d, 1 H,  $J = 14$  Hz); high-resolution mass spectral analysis for  $C_{18}H_{22}N_2O_3$  calcd 314.1630, found 314.1630.

**Cis-Trans Imide Amide Naphthalene 9b.** A solution of 75.0 mg (0.291 mmol) of **8b** in 2.0 mL of  $CH_2Cl_2$  was added to an ice cold solution of 129 mg (0.901 mmol, 3.1 equiv) of 2-aminonaphthalene in 2.0 mL of  $CH_2Cl_2$ , 1.25 mL of dry pyridine, and a catalytic amount of DMAP under  $N_2$ . After 1 h, the ice bath was removed and stirring continued for an additional 8 h. After workup and flash chromatography (described in **9a**), 79.7 mg of product **9b** (75.2% yield) was obtained as a colorless solid: mp 255–256 °C; IR, 3368, 3300, 1699, 1678, 1555, 1500  $cm^{-1}$ ;  $^1H$  NMR  $\delta$  8.21 (s, 1 H), 7.88 (d, 1 H,  $J = 7$  Hz), 7.79 (d, 1 H,  $J = 7$  Hz), 7.45 (m, 3 H), 7.30 (s, 1 H), 2.15 (d, 1 H,  $J = 14$  Hz), 2.05 (dd, 2 H,  $J = 7$  Hz), 1.50 (m, 3 H), 1.45 (s, 3 H), 1.25 (ns, 6 H); high-resolution mass spectral analysis for  $C_{22}H_{24}N_2O_3$  calcd 364.1787, found 364.1787.

**Cis-Trans Imide Amide Anthracene 9c.** A solution of 125 mg (0.485 mmol) of **8b** in 3.0 mL of  $CHCl_3$  was added to a stirred solution of 103 mg (0.533 mmol, 1.1 equiv) of purified 2-aminoanthracene and a catalytic amount of DMAP in 8.0 mL of dry pyridine at room temperature. The reaction was stirred under  $N_2$  for 10 h and then diluted with  $CH_2Cl_2$ . The solution was washed with 10% aqueous HCl and saturated aqueous  $NaHCO_3$ , dried ( $Na_2SO_4$ ), filtered, and concentrated. Purification of the product by flash chromatography on a 19-mm column using 25% EtOAc in hexanes afforded 149 mg (74.1% yield) as a slightly yellow

solid: mp > 300 °C; IR, 3337, 3244, 3100, 2924, 1670, 1550, 1377  $cm^{-1}$ ;  $^1H$  NMR  $\delta$  8.37 (d, 2 H,  $J = 7$  Hz), 8.36 (d, 2 H,  $J = 7$  Hz), 7.97 (dd, 2 H,  $J_1 = 7$  Hz,  $J_2 = 1$  Hz), 7.26 (s, 1 H), 2.70 (d, 1 H,  $J = 14$  Hz), 2.04 (q, 4 H,  $J = 7$  Hz), 1.45 (s, 3 H), 1.36 (s, 6 H), 1.35 (m, 3 H); high-resolution mass spectral analysis for  $C_{26}H_{26}N_2O_3$  calcd 414.1943, found 414.1945.

**Cis-Trans Imide Amide Anthraquinone 9d.** A solution of 96.8 mg (0.376 mmol) of imide acid chloride **8b** was added to an ice cold, magnetically stirred solution of 122 mg (0.546 mmol, 1.5 equiv) of purified 2-aminoanthraquinone and a catalytic amount of DMAP in 10.0 mL of dry pyridine under  $N_2$ . After 1 h, the ice bath was removed. Stirring was continued for 8 h, and then the reaction was diluted with  $CH_2Cl_2$ . The solution was washed with 10% aqueous HCl and saturated aqueous  $NaHCO_3$ , dried ( $Na_2SO_4$ ), filtered, and concentrated. Purification of the product by flash chromatography on a 19-mm column using 25% EtOAc in hexanes as eluent afforded 128 mg (76.6% yield) of **9d** as a slightly yellow solid: mp > 300 °C; IR, 3350, 3200, 2950, 1772, 1716, 1695  $cm^{-1}$ ;  $^1H$  NMR  $\delta$  8.31 (m, 5 H), 8.22 (d, 1 H,  $J = 1$  Hz), 7.83 (s, 1 H), 7.81 (m, 2 H), 7.58 (s, 1 H), 2.32 (d, 2 H,  $J = 14$  Hz), 2.15 (d, 2 H,  $J = 14$  Hz), 2.02 (d, 2 H,  $J = 14$  Hz), 1.58 (s, 6 H), 1.45 (s, 3 H), 1.30 (d, 1 H,  $J = 14$  Hz); high-resolution mass spectral analysis for  $C_{26}H_{24}N_2O_5$  calcd 444.1685, found 444.1685.

**Acknowledgment.** We are grateful to the National Science Foundation for support of this work.

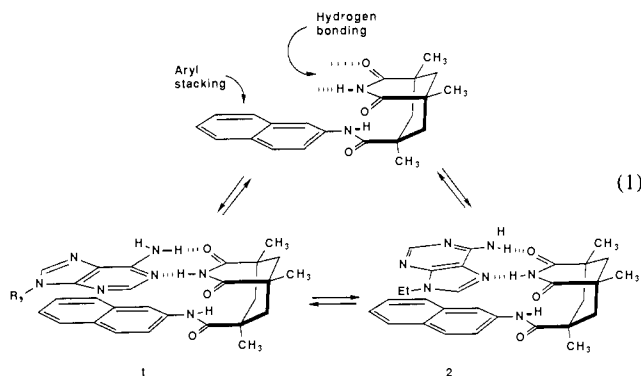
## Molecular Recognition with Convergent Functional Groups. 7. Energetics of Adenine Binding with Model Receptors

Kevin Williams, Ben Askew, Pablo Ballester, Chris Buhr, Kyu Sung Jeong, Sharon Jones, and Julius Rebek, Jr.\*

Contribution from the Department of Chemistry, University of Pittsburgh, Pittsburgh, Pennsylvania 15260. Received November 18, 1987

**Abstract:** The energetics of complexation for model receptors and adenine derivatives are reported. The new systems feature Watson-Crick, Hoogsteen, and bifurcated hydrogen bonding as well as aryl stacking interactions. These factors can act simultaneously on adenine derivatives because the model receptors present cleftlike shapes which are complementary to the surface of adenine. The association constants vary from 50 to  $10^4 M^{-1}$  in solvents such as  $CDCl_3$  that compete poorly for hydrogen bonds. The energetics of binding are explored as a function of receptor and guest structure, solvent, and temperature.

In the preceding paper we introduced a new type of receptor for adenine derivatives (eq 1) and gave evidence for structural features involved in its complexes.<sup>1</sup> The new systems are based



on the U-shaped relationship between functional groups provided by Kemp's<sup>2</sup> triacid **3**, a feature that permits simultaneous binding through base pairing and aromatic stacking interactions. These forces converge from perpendicular directions and provide an ideal

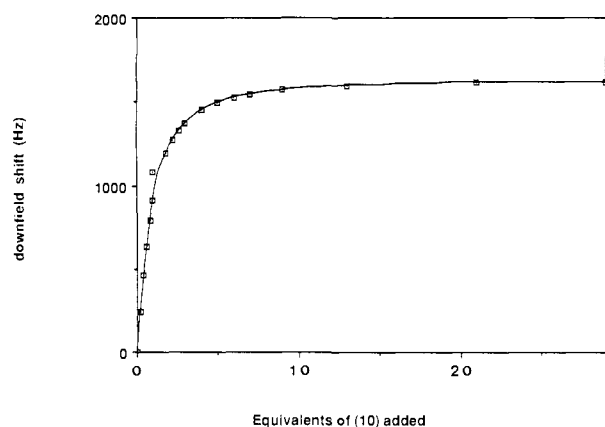
**Table I.** Association Constants and Degree of Saturation Observed for the Binding of **10** to the Model Receptors ( $CDCl_3$ , 24 °C)

entry	receptor	$K_a, M^{-1}$	satrn, %
1	<b>4c</b>	50	65
2	<b>4d</b>	50	69
3	<b>5a</b>	101	79
4	<b>5b</b>	220	86
5	<b>5c</b>	440	96
6	<b>5d</b>	210 <sup>a</sup>	96
7	<b>5e</b>	120 <sup>a</sup>	98
8	<b>5f</b>	90	79
9	<b>5g</b>	125	76
10	<b>5h</b>	79	78
11	<b>5i</b>	64	77
12	<b>5j</b>	11000	96
13	<b>5k</b>	2500	~100
14	<b>5l</b>	2300	~100
15	<b>5m</b>	206	74
16	<b>8c</b>	50	65
17	<b>9a</b>	66	70
18	<b>9b</b>	54	69
19	<b>9c</b>	59	70

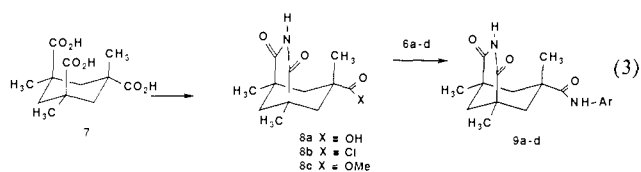
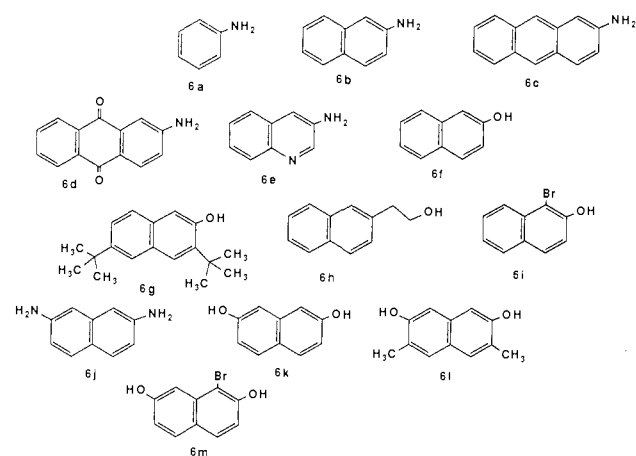
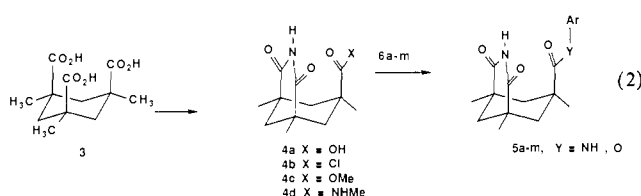
<sup>a</sup>Uncorrected for the presence of dimer.

microenvironment for adenine derivatives. In this paper we explore the energetics of the binding event as a function of structure, solvent, temperature, and substrate.

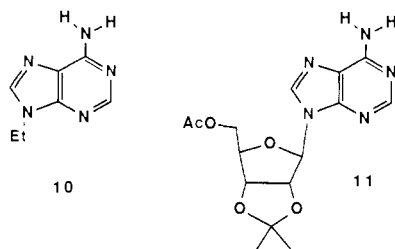
(1) B. Askew; P. Ballester; C. Buhr; K. S. Jeong; S. Jones; K. Parris; K. Williams; J. Rebek, Jr. *J. Am. Chem. Soc.*, preceding paper in this issue.  
(2) Kemp, D. S.; Petrakis, K. S. *J. Org. Chem.* 1981, 46, 5140-5143.

Figure 1. Saturation plot of **5c** titrated with **10**.

**Synthesis.** The synthesis of the systems involves acylation of **4b** with various amines and phenols (**6a-m**); the isomeric derivatives **9a-d** were prepared from **7** for comparison purposes (eq 2 and 3). The experimental details for the preparations are described in the preceding paper,<sup>1</sup> and the same numbering system for structures is used here.



**Methods.** Association constants were obtained by NMR titration protocols that generally involved addition of adenine derivatives **10** or **11** to solutions of the imides in  $\text{CDCl}_3$  or other



suitable NMR solvents. Complexation results in the downfield

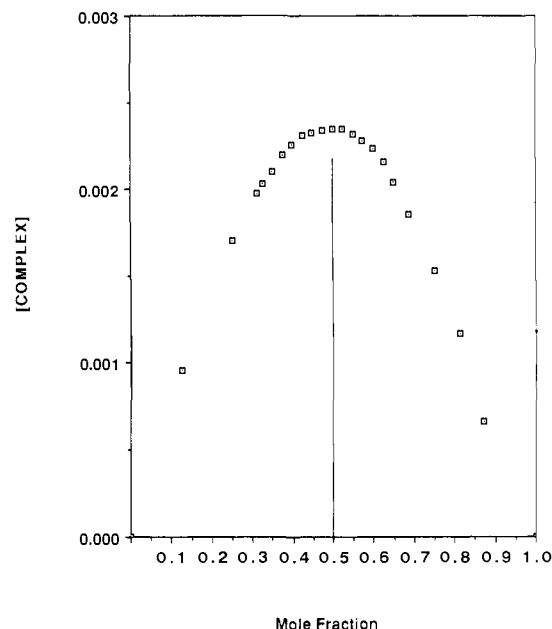
Figure 2. Job plot of **5c** and **10**.

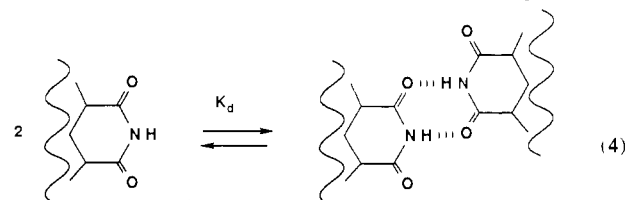
Table II. Self-Association (Dimerization) Constants (eq 4)

entry	receptor	$K_d$ , $\text{M}^{-1}$	entry	receptor	$K_d$ , $\text{M}^{-1}$
1	<b>5a</b>	2.8	4	<b>5d</b>	>50
2	<b>5b</b>	2.5	5	<b>5e</b>	59
3	<b>5c</b>	2.2	6	<b>8c</b>	2.0

shift of the imide NH signal from 7.6 to >13 ppm. Typical saturation data are shown in Figure 1 for the specific case of **5c** and 9-ethyladenine (**10**) in  $\text{CDCl}_3$  at room temperature. A Job plot for **5c**, reproduced in Figure 2, established that a 1:1 stoichiometry was involved.<sup>3</sup> Significantly, the diimides **5j** and **5k** gave Job plots that also showed maxima at 0.5 mole fraction, characteristic of a 1:1 complex.

There are a number of problems involved in evaluating titration data of this sort (a subject well-treated by Deranleau<sup>4</sup>), and for the most part, we have wrought the data with the Eadie method.<sup>5</sup> The association constants  $K_a$  are generally in the range of  $50 \rightarrow 10^3$ , so it is possible to observe the saturation range of  $20 \rightarrow 95\%$  for titrations at NMR concentrations. We estimate (based on reproducibility) that the numbers for the association constants are only good to  $\pm 10\%$ , even though some titrations gave results within 2% of each other. Generally, it took 30 equiv of 9-ethyladenine to reach the limiting NMR spectrum, in which the chemical shift of the imide reaches ca. 13–13.5 ppm. Even in those cases where the limit was not reached, it is still reasonable to assume that saturation results in the same chemical shift for the imide NH involved in base pairing. The value of 13.2 was used to determine the degree of saturation. Table I gives the results for the various structures.

Self-association of these systems is possible since complementary hydrogen bonds can be formed in imide dimers<sup>6</sup> (eq 4). An

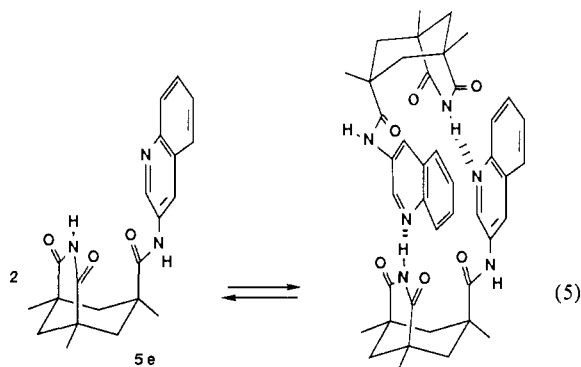


estimate can be made for the dimerization constant  $K_d$ , based on

(3) Conner, K. *Binding Constants*, Wiley: New York, 1987.(4) Deranleu, D. A. *J. Am. Chem. Soc.* **1969**, *91*, 4044.(5) Eadie, G. S. *J. Biol. Chem.* **1942**, *146*, 85–93.(6) Kyogoku, Y.; Lord, R. G.; Rich, A. *Proc. Natl. Acad. Sci. U.S.A.* **1967**, *57*, 250–257. Hine, J.; Hahn, S.; Hwang, S. *J. Org. Chem.* **1988**, *53*, 884–887.

the change in chemical shift of the imide NH resonance with concentration. For such very low association constants, neither the saturation nor the infinite dilution limit can be reached experimentally, and the determination is fraught with error.<sup>7</sup> Even so, we estimate the values in Table II for representative systems. These are calculated by using a limiting chemical shift of 10.2 ppm for the imide dimer; this value is based on our experience with cyclic systems.<sup>8</sup> The systems generally show  $K_d$ 's in the 2–4  $M^{-1}$  range, values that are consistently negligible. Accordingly, our reported  $K_a$ 's are uncorrected for these effects.

An exception is the quinoline derivative **5e**. With a program developed by Wilcox,<sup>9</sup> a  $K_d$  of 59  $M^{-1}$  was calculated for this case (Table II, entry 5). This high degree of association is most likely the result of the stacking interactions that are simultaneously available with hydrogen bonding in this system, eq 5. Since such



“self-complementarity” is an inevitable feature of many heterocyclic systems, we have avoided their use in adenine-recognition studies. Even the quinone **5d** showed some evidence of dimerization (Table II, entry 4). However, solubility problems made a survey of its self-association difficult and our subsequent binding experiments with it are less precise as a result. Such molecular systems have special applicability to the problems involved in self-recognition and self-replication, and we are continuing efforts to develop models for this phenomenon.

**Effects of Aryl Stacking.** One of the simplest trends that can be recognized involves the effect of surface *area* on the complexation event. In structures such as **5a–d**, hydrogen bonding is expected to contribute a constant amount but the different aromatic surfaces offer various degrees of  $\pi$ -stacking stabilization. The trends reflect mostly the increased polarizability of the larger aromatic surfaces leading ultimately to the van der Waals interactions or dipole-induced dipole interaction between the two components. The reduced efficiency of binding to the quinone **5d** was surprising, given the well-documented ability of anthraquinone type antibiotics to intercalate into intact double-stranded DNA.<sup>10</sup> The failure of the quinone to offer binding enhancements in this setting is due to its competing dimerization. An additional factor may be its own dipole. The orientation of that dipole may not be optimal for interaction with that of the hydrogen-bonded adenine held nearby. Conversely, well-placed substituents on a neighboring aromatic surface may be expected to enhance the  $\pi$  stacking. In the absence of a good model for the charge distribution in the base-pairing part of the model, it is hard to predict an optimal aromatic surface for this interaction.

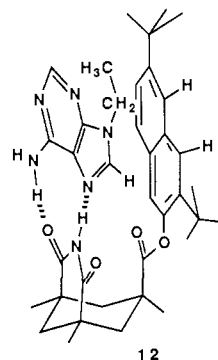
The nature of the stacking interaction is also exposed in the direct comparison of the two esters, the di-*tert*-butyl **5g** vs the unsubstituted naphthyl system **5f**. It was established in the previous paper<sup>1</sup> that the aromatic esters do not exhibit bifurcated hydrogen bonding with adenine; the differences between **5f** and **5g** must arise from differences in aromatic stacking capabilities. (The effect of a seemingly remote *tert*-butyl group on the strength

**Table III.** Association Constants for Receptors in Contact with **10** and **13** ( $CDCl_3$ , 24 °C)

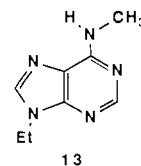
entry	receptor	$K_a$ , $M^{-1}$	
		<b>10</b>	<b>13</b>
1	<b>5b</b>	220	115
2	<b>5c</b>	440	142
3	<b>5f</b>	90	45
4	<b>5g</b>	125	88

of the hydrogen bonds is hard to evaluate but is assumed to be negligible.<sup>11)</sup>

The NOE experiments<sup>1</sup> lead to the interpretation that the *tert*-butyl derivative prefers largely the Hoogsteen mode of interaction as in **12**, whereas no differences between Watson–Crick



and Hoogsteen can be observed for the corresponding unsubstituted ester. It is also possible to compare the binding of the *N*-methylated adenine **13**, which strongly favors Hoogsteen base pairing,<sup>12</sup> to these two substrates (Table III).



It is seen that the  $K_a$  with **13** and **5b** is reduced by ~50% from the value for the simple adenine **10**. This suggests that roughly equal amounts of Watson–Crick and Hoogsteen modes are operating with 9-ethyladenine (**10**) when it is in contact with a naphthalene surface (Table III, entries 1 and 3). The positions of the *t*-Bu groups in **5g** favor Hoogsteen base pairing to the extent that 70% of the base pairing was estimated to be Hoogsteen from NOE results.<sup>13a</sup> With *N*-methyladenine, the  $K_a$  is indeed reduced only by ~25% (Table III, entry 4), i.e., the Watson–Crick mode of base pairing is apparently eliminated while the Hoogsteen mode remains unaffected. At the other extreme, the anthryl surface provides better overlap with the more extended, Watson–Crick arrangement. Accordingly, *N*-methylation causes a 60% decrease in  $K_a$  with **5a** (Table III, entry 2).

For base pairing alone, either the methyl ester **4c** or the divergent compounds **9a–e** may be used as standards, since only hydrogen bonding can contribute to complex stabilization. For the ester **4c**  $K_a = 50 M^{-1}$ , while for **9a–c**  $K_a = 65 \pm 6 M^{-1}$ . Remarkably, the amide **4d** also gave  $K_a = 50 M^{-1}$ . For comparison purposes, an IR study of Rich<sup>6</sup> involving cyclohexyluracil and **10** in  $CDCl_3$  gave  $k_a = \sim 100 M^{-1}$ , whereas the corresponding value

(11) For a discussion of proton transfers aided by stacking interactions in biological systems, see: Osman, R.; Topiol, S.; Rubenstein, L.; Weinstein, H. *Mol. Pharm.* **1987**, *32*, 699–705. For the effects of charge on aryl stacking, see: Ishida, T.; Doi, M.; Ueda, H.; Inoue, M.; Scheldrick, G. M. *J. Am. Chem. Soc.* **1988**, *110*, 2286–2294.

(12) Saenger, W. *Principles of Nucleic Acid Structure*; Springer-Verlag: New York, 1984; Chapter 6. Dodin, G.; Dreyfus, M.; Dubois, J.-E. *J. Chem. Soc., Perkin Trans. 2* **1979**, 439.

(13) (a) Rebeck, J., Jr.; Williams, K.; Parriss, K.; Ballester, P.; Jeong, K.-S. *Angew. Chem., Int. Ed. Engl.* **1987**, *26*, 1244–1245. (b) Sowers, L. C.; Shaw, B. R.; Sedwick, W. D. *Biochem. Biophys. Res. Commun.* **1987**, *148*, 790–794.

(7) Horman, I.; Dreux, B. *Helv. Chim. Acta* **1984**, *67*, 754–764.

(8) Tjivikua, T.; Rebeck, J., Jr., manuscript in preparation.

(9) Wilcox, C. S.; Cowart, M. D. *Tetrahedron Lett.* **1986**, *27*, 5563–5566.

(10) Quigley, G. J.; Wang, A. H.-J.; Ughetto, G.; van der Marcel, G.; van Boom, J. H.; Rich, A. *Proc. Natl. Acad. Sci. U.S.A.* **1980**, *77*, 7204–7208.

**Table IV.** Association Constants of Model Receptors Titrated with **10** and **11**

entry	substrate	$K_a, M^{-1}$	
		<b>11</b>	<b>10</b>
2	<b>5g</b>	88	125
3	<b>5k</b>	2100	2500
4	<b>5l</b>	1900	2300

**Table V.**

solvent	$K_{anth}(\mathbf{5c})$	$K_{phe}(\mathbf{5a})$	ratio
$CDCl_3$	440	100	4.4
50% $CD_3CN-CDCl_3$	82	26	3.2
$CD_3OD$	41	11	3.7

with *dihydrouracil* and the adenine derivative was  $30 M^{-1}$ . Thus a "typical" value is hard to establish for base pairing.

A second factor influencing the relative properties of Watson-Crick and Hoogsteen base pairing is the orientation of the aromatic stacking surface. Relatively extended aromatics such as the anthracene **5c** provide better overlap for the Watson-Crick mode, while larger proximal surfaces are expected to favor Hoogsteen binding. The enhanced binding of the *tert*-butyl group of **5g** is outside the range attributable to experimental error, and we believe that this is due to the *polarizability* of the added *tert*-butyl groups. In contact with adenine, the entire naphthalene surface responds with a greater stacking stabilization.<sup>13a</sup> This interpretation is consistent with the larger intermolecular NOEs observed for the *tert*-butyl vs the unsubstituted in contact with adenines and recent results of Sowers.<sup>13b</sup> Additional support is provided by some of the thermodynamic parameters discussed below.

A direct comparison between complexation of 9-ethyladenine (**10**) and the ribose derivative **11** was also staged. The results (Table IV) reveal that the affinity of either derivative for the model receptors is comparable. Nothing sinister or unusual is introduced by the use of the simpler side chain in this study, and the 20% or so diminution of affinity for the ribose derivative can be attributed to steric effects.

**Solvation.** The intrinsic features of the stacking interaction were the object of studies in various solvents. Desolvation is an important part of aryl-aryl interactions in hydroxylic media.<sup>14</sup> If such hydrophobic effects are the driving force for stacking, it would be expected that larger surfaces would be more prone to stacking because of their entropic advantage of releasing more bound solvent to the bulk medium. Direct comparisons between the smaller phenyl and the larger anthryl surfaces were made in a number of suitable solvent mixtures. The results (Table V) indicate a *constancy of the effect of stacking*. Even in the hydroxylic medium, methanol, no special enhancement of the larger surface is observed. The release of organized methanol to bulk solvent, an entropically favored process, does not seem to be a major contributor to the driving force of these aromatic stacking interactions.

**Thermodynamics.** The thermodynamic parameters were obtained from temperature-dependent studies using van't Hoff plots. Direct competitions were performed in several of these studies and the average value of three determinations is reported in Table VI. Again, the assumption of a temperature-independent chemical shift for the fully complexed imide NH resonance was made. It is observed that both  $\Delta H$  and  $\Delta S$  are larger in magnitude for the larger surface than for the smaller surface. While this may be yet another expression of the curious compensation of  $\Delta H$  and  $\Delta S$ , it may also reflect a "tighter" binding in both enthalpic and entropic senses for the larger surface.

The magnitude of  $\Delta H$  is quite reasonable given the types of hydrogen bonds involved. The base pairing contributes about 6 or 7 kcal/mol in the relatively noncompeting solvent  $CDCl_3$ , and

(14) For leading references, see: Menger, F. M.; Whitesell, L. G. *J. Org. Chem.* **1987**, *52*, 3793-3798. Ravishanker, G.; Beveridge, D. L. *J. Am. Chem. Soc.* **1985**, *107*, 2565-2566.

**Table VI.**

binding to	$K, 296 K, M^{-1}$	$-\Delta H, kcal/mol$	$-\Delta S, eu$
amides			
phenyl ( <b>5a</b> )	100	8.75	19
naphthyl ( <b>5b</b> )	220	9.45	21
anthracyl ( <b>5c</b> )	440	12.5	30
esters			
naphthyl ( <b>5f</b> )	90	7.7	17
di- <i>t</i> -Bu-naphthyl ( <b>5g</b> )	125	8.7	19.5

**Table VII.** Experimental Parameters for NMR Titrations

entry	receptor	initial concn host:guest	equiv added	obsd shift, ppm
1	<b>4c</b>	0.0076:0.08	30.8	11.3
2	<b>4d</b>	0.01:0.1	37.2	11.5
3	<b>5a</b>	0.01:0.1	11.0	12.1
4	<b>5b</b>	0.012:0.073	9.0	12.4
5	<b>5c</b>	0.01:0.077	9.0	13.0
6	<b>5d</b>	0.01:0.070	22.0	13.0
7	<b>5e</b>	0.02:0.0068	15.0	13.0
8	<b>5f</b>	0.01:0.1	30.0	12.0
9	<b>5g</b>	0.01:0.1	50.0	11.8
10	<b>5h</b>	0.01:0.1	33.2	11.9
11	<b>5i</b>	0.01:0.1	28.2	11.9
12	<b>5j</b>	0.00175:0.075	4.5	13.0
13	<b>5k</b>	0.01:0.1	10.0	13.2
14	<b>5l</b>	0.01:0.1	2.0	13.2
15	<b>5m</b>	0.005:0.05	27.2	11.7
16	<b>8c</b>	0.01:0.1	50.0	11.5
17	<b>9a</b>	0.01:0.1	12.0	11.5
18	<b>9b</b>	0.01:0.1	31.0	11.4
19	<b>9c</b>	0.01:0.1	31.8	11.5

this figure is within the ranges set by literature precedent.<sup>15</sup> Assuming that the quality and type of hydrogen bonds formed with the anthryl surface is the same as that with the phenyl surface, the difference of nearly 4 kcal in  $\Delta H$  must result from the aromatic stacking interactions. The difference in  $\Delta S$  of  $\sim 11$  eu resists this binding force; entropy is reduced to a greater extent with the larger surface. This should not be due merely to the symmetry changes, as they are expected to contribute only a small amount to the figures. Rather, the results indicate that motions within the complex, perhaps involving low-frequency vibrations, are more reduced in the larger surface compared to those in the smaller ones.<sup>16</sup> Stacking to the larger surfaces is entropically *disfavored* but enthalpically *avored*. The net result is a  $\Delta\Delta G$  of  $\sim 1$  kcal/mol observed between the two aromatic surfaces, anthryl vs phenyl.

In conclusion, we have explored how model systems can be used as a probe for the energetics of hydrogen bonding and aryl stacking interactions, forces that stabilize double-stranded DNA. While our systems are some distance from biorelevance because of their low water solubility, we have recently observed binding of the adenine derivatives, ATP, NADH, etc, in water-methanol mixtures. With the chelating systems, transport of adenosine through liquid membranes can also be demonstrated.<sup>17</sup> We will report on these experiments in due course.

### Experimental Section

(1) **Materials.** The structures of this study were prepared and characterized as described in ref 1.

(2) **Methods for the Evaluation of Association Constants.** (a) **Self-Association.** Typically, before any complexation reactions were studied, self-association of the host was examined. Generally, a concentrated solution of the host (saturation limit) was diluted, and a change in an

(15) Pohorille, A.; Burt, S. K.; MacElroy, R. D. *J. Am. Chem. Soc.* **1984**, *106*, 402-409.

(16) For related studies involving aryl-aryl interactions with cyclophane derivatives in a variety of solvents, see: Diederich, F.; Dick, K.; Griebel, D. *J. Am. Chem. Soc.* **1986**, *108*, 2273-2286. Ferguson, S. B.; Diederich, F. *Angew. Chem., Int. Ed. Engl.* **1986**, *25*, 1127-1129. Diederich, F. *Ibid.* **1988**, *27*, 362-386.

(17) Benzing, T.; Tjiuikua, T.; Wolfe, J.; Rebek, J., Jr. *Science* **1988**, *242*, 266-268.

analytical response was observed. The analytical response in all of these studies was an upfield or downfield shift of a  $^1\text{H}$  NMR resonance peak; specifically, the upfield shift of the imide NH proton was observed on dilution. If a minimal change in chemical shift ( $<0.5$  ppm) was observed through a large range of concentrations ( $0.25\text{--}10^{-5}$  M) it was concluded that the self-association was negligible. For a reference study the cis-trans methyl ester derivative **8c** was concentrated to 1.25 M (268 mg/mL) and cooled to 230 K, at which temperature the chemical shift of the imide NH proton ceased to change (9.8 ppm). This value was subsequently used as the intrinsic chemical shift of the hydrogen-bonded dimer, and 7.6 ppm was used as the chemical shift of the free imide NH. By using these end points, self-association constants of Table II were calculated for these receptors (**5a-e**, **8c**).

(b) **Stoichiometry.** The complexes with adenine derivatives (**10**, **11**, **13**) were determined to be of 1:1 stoichiometry by using Job's method<sup>3</sup> (Figure 2). For a specific case, the Job plot of **5k** and **10** is described here in detail. Solutions of **5k** and **10** (0.01 M each) were made in separate volumetric flasks. In nine separate 5-mm-o.d. NMR tubes mixtures of each solution were added such that the stoichiometry of each component varied but the total volume was 500  $\mu\text{L}$ . For example, the first tube contained only the receptor; the second tube contained 5  $\mu\text{L}$  of the solution of **5k** and 495  $\mu\text{L}$  of the solution of **10**. Likewise, the last tube contained only the ligand, and the tube before that contained 495  $\mu\text{L}$  of the solution of **5k** and 5  $\mu\text{L}$  of the solution of **10**. The  $^1\text{H}$  NMR spectra were obtained for each tube, and the chemical shift of the imide NH proton was used to calculate the complex concentration. This value was plotted against the mole fraction of the **5k**. The resulting Job plot showed a maximum at 0.5 mole fraction (see Figure 2b).

(c) **Titrations.** For a specific example, the titration of **5g** with **10** will be described here. A 0.01 M solution of **5g** (4.77 mg in 1 mL of  $\text{CDCl}_3$ ) and a 0.1 M solution of **10** (32.6 mg in 1 mL of  $\text{CDCl}_3$ ) were prepared in separate 1-mL volumetric flasks. A 500- $\mu\text{L}$  portion of the solution of **5g** was added to a 5-mm-o.d. NMR tube. An initial NMR spectrum was obtained, and the initial chemical shift of the imide NH proton was 7.78 ppm at this concentration. The guest was initially added in 10- $\mu\text{L}$  portions, and the chemical shift of the imide proton was recorded at each increment. (Care was taken to recover the stock solution of guest to prevent evaporation, which causes significant deviations in the resulting Eadie plots.) After 60  $\mu\text{L}$  ( $\sim 1$  equiv) of guest had been added, the

aliquot size was increased to 20  $\mu\text{L}$ . After 200  $\mu\text{L}$  had been added the aliquot size was increased to 50  $\mu\text{L}$  until 500  $\mu\text{L}$  was added, then 100- $\mu\text{L}$  aliquots were added until 1000  $\mu\text{L}$  of guest had been added, and finally 250- $\mu\text{L}$  portions were added until 1750  $\mu\text{L}$  (35 equiv) of the guest had been added. The chemical shift of the imide NH proton at this concentration of guest was 12.8 ppm. The experiment was repeated three additional times to give  $K_a = 125 \pm 8 \text{ M}^{-1}$ . Typically, 20-30 equiv of guest was needed for the chemical shift of the imide NH proton to reach saturation. The value 13.2 ppm was experimentally determined to be the maximal chemical shift by cooling a 2:1 solution of **10** and the chelating molecule **5h** below the coalescence temperature ( $\sim 210$  K), at which temperature the chemical shift of the imide NH proton was 13.2 ppm. This value was used in all subsequent titrations, especially those for which it was not experimentally possible to reach the limiting chemical shift of the imide NH proton.

(d) **Thermodynamic Studies.** An equimolar solution of **5k** and **10** were made up in a volumetric flask by using 6.30 mg of **5k** and 1.63 mg of **10** in 2 mL of  $\text{CDCl}_3$ . A 500- $\mu\text{L}$  portion of this solution was added to a 5-mm-o.d. NMR tube and cooled to 273 K. The chemical shift of the imide NH proton was recorded at this temperature and at every 5 K temperature increment as the sample was warmed to 323 K (equilibrium time at each temperature was 5 min.). The van't Hoff plots of the  $K_a$ 's calculated at each temperature gave  $-\Delta H$  and  $-\Delta S$ . In order to ensure that a reasonable range of the saturation plot was covered, the initial solution concentration was adjusted such that, over the range of temperatures studied,  $0.2 \leq$  fraction saturation  $\leq 0.8$  was maintained.

**Acknowledgment.** We are pleased to acknowledge financial support from the National Science Foundation for this work, and we thank Professor C. S. Wilcox for help with his curve-fitting program.

**Registry No.** **4c**, 109216-51-5; **4d**, 117873-87-7; **5a**, 109216-52-6; **5b**, 109216-53-7; **5c**, 109216-54-8; **5d**, 109216-55-9; **5e**, 117873-88-8; **5f**, 111689-17-9; **5g**, 111635-64-4; **5h**, 117873-89-9; **5i**, 117873-90-2; **5j**, 117873-91-3; **5k**, 117873-92-4; **5l**, 117895-86-0; **5m**, 117873-93-5; **8c**, 117873-94-6; **9a**, 117873-95-7; **9b**, 117873-96-8; **9c**, 117873-97-9; **10**, 2715-68-6; **11**, 15888-38-7; **13**, 21031-78-7;  $\text{CDCl}_3$ , 865-49-6;  $\text{CD}_3\text{CN}$ , 2206-26-0;  $\text{CD}_3\text{OD}$ , 811-98-3.

## Structure and Acid-Base Properties of One-Electron-Oxidized Deoxyguanosine, Guanosine, and 1-Methylguanosine

L. P. Candeias<sup>1</sup> and S. Steenken\*

Contribution from the Max-Planck-Institut für Strahlenchemie,  
D-4330 Mülheim, Federal Republic of Germany. Received July 13, 1988

**Abstract:** Deoxyguanosine, guanosine, and 1-methylguanosine react in aqueous solution with  $\text{SO}_4^{\cdot-}$  with nearly diffusion-controlled rates and with  $\text{Br}_2^{\cdot-}$  with rate constants close to  $\approx 5 \times 10^7 \text{ M}^{-1} \text{ s}^{-1}$ . The resulting radical cations have  $\text{p}K_a$  values of 3.9 and 4.7 for the nonmethylated and methylated systems, respectively, so that at pH 7 the products of one-electron oxidation are neutral radicals, formed by deprotonation from N(1) in the case of guanosine and deoxyguanosine and from the exocyclic N<sup>2</sup> in the case of 1-methylguanosine. The radicals of deoxyguanosine and guanosine, but not that from 1-methylguanosine, further deprotonate to give radical anions with  $\text{p}K_a$  values of 10.8 and 10.7, respectively. An implication of these results to the radiation chemistry of DNA is that the radical cation formed upon ionization of a guanine moiety shifts a proton (and thereby a positive charge) to its complementary base cytosine, i.e., that separation of charge from spin occurs by proton transfer.

Guanine has been known for a long time to be the most easily oxidized of the nucleic acid bases.<sup>2</sup> This property is in line with (gas-phase) ionization potential<sup>3</sup> as well as aqueous solution redox

potential data,<sup>4</sup> and it is in accord with the results of MO calculations.<sup>5</sup> In agreement with this concept, the guanine moiety appears to be the ultimate trap of oxidative damage to DNA, as concluded from ESR data on "dry" DNA, irradiated frozen solutions,<sup>6</sup> and oriented DNA fibers.<sup>7</sup> These data have so far been

(1) Part of the Ph.D. work to be presented at Instituto Superior Tecnico P-1096 Lisboa, Portugal.

(2) For a review on purine radical chemistry, see: Steenken, S. *Chem. Rev.*, in press.

(3) Hush, N. S.; Cheung, A. S. *Chem. Phys. Lett.* **1975**, *34*, 11. McGlynn, S. P.; Dougherty, D.; Mathers, T.; Abdulner, S. In *Excited States in Organic Chemistry and Biochemistry*; Pullman, B., Goldblum, N., Eds.; D. Reidel: Dordrecht, 1977; p 247.

(4) Jovanovic, S. V.; Simic, M. G. *J. Phys. Chem.* **1986**, *90*, 974.

(5) Pullman, B.; Pullman, A. *Quantum Biochemistry*; Interscience Publishers: New York, 1963. Berthod, H.; Giessner-Prettre, C.; Pullman, A. *Theor. Chim. Acta* **1966**, *5*, 53. Bodor, N.; Dewar, M. J. S.; Harget, A. J. *J. Am. Chem. Soc.* **1970**, *92*, 2929. Rakvin, B.; Herak, J. N. *Radiat. Phys. Chem.* **1983**, *22*, 1043.